Modeling of non-stationary local response on impurity penetration in plasma

M. Z. Tokar and M. Koltunov

Citation: Phys. Plasmas **19**, 042502 (2012); doi: 10.1063/1.3701555
View online: http://dx.doi.org/10.1063/1.3701555
View Table of Contents: http://pop.aip.org/resource/1/PHPAEN/v19/i4
Published by the American Institute of Physics.

Modeling of non-stationary local response on impurity penetration in plasma

M. Z. Tokar and M. Koltunov
Institut für Energie- und Klimaforschung—Plasmaphysik, Forschungszentrum Jülich GmbH, EURATOM Association, Trilateral Euregio Cluster, D-52425 Jülich, Germany

(Received 14 December 2011; accepted 21 February 2012; published online 12 April 2012)

In fusion devices, strongly localized intensive sources of impurities may arise unexpectedly, e.g., if the wall is excessively demolished by hot plasma particles, or can be created deliberately through impurity seeding. The spreading of impurities from such sources both along and perpendicular to the magnetic field is affected by coulomb collisions with background particles, ionization, acceleration by electric field, etc. Simultaneously, the plasma itself can be significantly disturbed by these interactions. To describe self-consistently the impurity spreading process and the plasma response, three-dimensional fluid equations for the particle, parallel momentum, and energy balances of various plasma components are solved by reducing them to ordinary differential equations for the time evolution of several parameters characterizing the solutions in principal details: the maximum densities of impurity ions of different charges, the dimensions both along and across the magnetic field of the shells occupied by these particles, the characteristic temperatures of all plasma components, and the densities of the main ions and electrons in different shells. The results of modeling for penetration of lithium singly charged particles in tokamak edge plasma are presented. A new mechanism for the condensation phenomenon and formation of cold dense plasma structures, implying an outstanding role of coulomb collisions between main and impurity ions, is proposed. [http://dx.doi.org/10.1063/1.3701555]

I. INTRODUCTION

Due to destruction of machine walls, impurities unavoidably get into plasmas of fusion devices.[1] Moreover, some impurity species are seeded deliberately, e.g., to analyse and modify transport properties, to study the routes and transport mechanisms of particles released from the walls, to create strongly radiating plasma mantle for cooling down the plasma edge and weakening plasma-wall interactions, to soften harmful consequences of disruptive instabilities, etc.[2–6] The main interest of such experiments is of course the impact of impurities on the global plasma behavior. Nonetheless, the local plasma response, i.e., in the direct vicinity of the impurity entrance position, can be also relevant for global effects. Indeed, the ionization of impurity supplies to the plasma new electrons, energy losses on excitation and heating of impurity particles can lead to a significant cooling of the main plasma components. As a result, the actual conditions in the plasma region where impurity neutral jet penetrates into the plasma may differ very strongly from those presumed there on the basis of experimental measurements performed normally far away from the injection position. These changes affect the impurity penetration process itself and, therefore, it has to be self-consistently treated by taking into account the plasma local response. There are several sophisticated code packages for self-consistent modeling of impurity transport and impacts in fusion plasmas, e.g., B2-EIRENE (Ref. 7) and EMC3-EIRENE (Ref. 8). However, the applicability of these and similar modeling tools in their present "state of the art" to situations in question is principally limited by the necessity to take into account (i) the essentially three-dimensional geometry of phenomena, (ii) the presence of physical processes with very different time scales, from 10^{-9} to 10^{-1} s, demanding non-stationary calculations with a time step as small as 10^{-10}s and a total number of steps of $10^8 - 10^9$, (iii) such physical processes as the heat exchange through coulomb collisions between different charged components, including impurity ions with a very low initial temperature. Although the code EMC3-EIRENE has been especially designed to handle three-dimensional configurations, presently it is not adapted for non-stationary calculations and nonidentical temperature of different ion species.

Another line of thinking is followed in Refs. 9–11 and allows to comply with the requirements above at the cost of the loss of the solution detailed spatial structure. Alternatively, to describe roughly this structure, approximate analytical expressions are used. These are constructed by taking into account that the competition between spreading of impurity ions of a given charge from the source and vanishing by ionization controls the dimensions of the shell occupied with the species in question. The time evolution of these dimensions is governed by equations obtained by integrating the three dimensional transport equations over some subregions of the shell. For diffusive spreading in one direction, the shell extension approaches to $\sqrt{D/(k_{ion}n_e)}$ in a final steady state, where D is the diffusivity, k_{ion} is the ionization rate coefficient, and n_e is the electron density.[12]

The locality of phenomena in question implies that the characteristic distances from the position of impurity entrance are significantly smaller than the device dimensions. Therefore, the particular geometry of the device should not play an essential role for the transport processes in the region under consideration. In particular, we neglect the effects of the ∇B and curvature drifts, which are important in the dynamics of other scrape-off layer (SOL) phenomena such as

"blobs."[13] For higher charged impurity ions distributed more homogeneously on magnetic surfaces, these toroidal effects may be more essential. Henceforce, we use an orthogonal reference system (x, y, z) with the coordinates x directed across the magnetic surfaces towards the plasma core, y aligned on the surface perpendicular to the magnetic field that is oriented in the direction z. The impurity ion transport in the directions x and y is assumed to be a diffusion with the diffusivity components D_x and D_y, respectively, and the impurity motion along the field is considered explicitly by solving momentum balance equations. An approximate "shell" approach to solve non-stationary three-dimensional equations for transport of low charged impurity ions spreading out from a local source has been developed in Refs. 10 and 11. In the present paper, we elaborate this approach further by including non-stationary description of the heat and particle balances for electrons and main plasma ions that allows to investigate the local plasma response on impurity penetration and to model these phenomena self-consistently.

In real experiments, the gas nozzle is often located in the shadow of a limiter or (and) beyond the magnetic separatrix. The injected neutrals and generated ions of impurity penetrate through the regions outside and inside the last closed flux surface (LCFS) with quite different plasma conditions.[14] Moreover, in the former case, the plasma loss to the limiter or target plate significantly affects the parallel motion of the main and impurity plasma components.[15] Under stationary conditions, this region has been studied in Refs. 9 and 16. Here, we consider the situation where the outlet of the injection valve defines itself the LCFS and impurities are spreading out in the confined region inside the LCFS, see Fig. 1. The impact of scrape-off layer outside the LCFS is taken into account as a boundary condition. This constraint does not allow to figure out the role of impurity ions produced in the SOL and penetrating into the confined region. The role of the latter has to be considered in future.

It is supposed that without impurity the plasma is homogeneous and motionless on magnetic surfaces. The impurity neutral density is assumed constant within the whole region of their localization, black rectangular area in Fig. 1. This model is simpler than that used in Refs. 9 and 10, in which the neutral density was decaying in the direction x. This simplification is made to construct approximate analytical solutions but it is not very essential for the results since (i) only the total number of neutrals prescribed by their influx from the valve, see Ref. 9, is of importance for the present model and (ii) the radial extension of the neutral jet is normally smaller than the thickness of the ion shells.[10] In spite that the present model is quite simplistic, and many *ad-hoc* approximations are made, it has reproduced quite accurately[9] the threshold for the development of cold edge plasma by methane puffing into TEXTOR.[17]

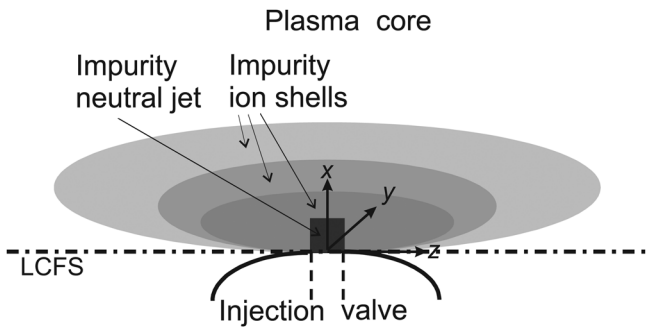

FIG. 1. Schematic view of shell regions occupied by different charged states of injected impurity.

The remainder of the paper is organized as follows. In Sec. II, fluid equations used to model the transport of impurity and plasma particles, their momentum along the magnetic field and thermal energy are presented. In Sec. III, a "shell" model is applied to reduce these three-dimensional nonstationary partial differential equations to ordinary ones, describing the time evolution of several characteristic parameters. The results of calculations for spreading of lithium particles at the edge of deuterium plasma in a tokamak are presented in Sec. IV. Finally, a new scenario for condensation instability and formation of cold dense structures in hot plasmas locally polluted by impurities is put forward.

II. BASIC EQUATIONS

The evolution with time t of the density n_j of impurity ions with the charge j and mass m is governed by a continuity equation[18]

$$\frac{\partial n_j}{\partial t} - \frac{\partial}{\partial x}\left(D_x \frac{\partial n_j}{\partial x}\right) - \frac{\partial}{\partial y}\left(D_y \frac{\partial n_j}{\partial y}\right) + \frac{\partial \Gamma_j}{\partial z} = k_{ion}^{j-1} n_e n_{j-1} - k_{ion}^{j} n_e n_j, \quad (1)$$

where k_{ion}^{j-1} and k_{ion}^{j} are the ionization rate coefficients and n_e is the electron density; owing to plasma quasi-neutrality,

$$n_e = n_i + \sum_j j n_j, \quad (2)$$

with n_i being the density of the main plasma ions. The density of the impurity ion flux component Γ_j parallel to the magnetic field is determined by the momentum balance equation

$$m\frac{\partial \Gamma_j}{\partial t} - m\frac{\partial}{\partial x}\left(\frac{D_x}{n_j}\frac{\partial n_j}{\partial x}\Gamma_j\right) - m\frac{\partial}{\partial y}\left(\frac{D_y}{n_j}\frac{\partial n_j}{\partial y}\Gamma_j\right) + m\frac{\partial}{\partial z}\left(\frac{\Gamma_j^2}{n_j}\right) = m(k_{ion}^{j-1}\Gamma_{j-1} - k_{ion}^{j}\Gamma_j)n_e + mk_{ij}(\Gamma_i n_j - \Gamma_j n_i) - \frac{\partial (n_j T_j)}{\partial z} + jeE_z n_j - F_{th}^{ej} - F_{th}^{ij}. \quad (3)$$

Here, k_{ij} is the friction coefficient due to coulomb collisions with the background ions[19] and Γ_i is flux density of the latter. The third term in the right hand side (rhs) is due to the pressure gradient where the impurity ion temperature T_j is controlled by the heat balance equation

$$\frac{3}{2}n_j\frac{\partial T_j}{\partial t} + T_j\frac{\partial \Gamma_j}{\partial z} = \frac{3}{2}(T_{j-1} - T_j)k_{ion}^{j-1} n_e n_j + 3n_j[k_{ij}n_i(T_i - T_j) + k_{ej}n_e(T_e - T_j)], \quad (4)$$

with T_i and T_e being the temperatures of the main ions and electrons, respectively, and k_{ej} characterizing coulomb

collisions between the latter and impurity. The last term in the rhs of Eq. (3) is the force due to electric field; its component parallel to the magnetic field, E_z, arises in the presence of a parallel gradient in the electron pressure. By neglecting electron inertia, one has a force balance

$$\partial(n_e T_e)/\partial z = -e n_e E_z + F_{th}^{ei} + \sum_j F_{th}^{ej}. \tag{5}$$

In Eqs. (3) and (5), $F_{th}^{ei} = -\alpha_{ei} n_e \partial T_e/\partial z, F_{th}^{ej} = -\alpha_{ej} n_e \partial T_e/\partial z$, and $F_{th}^{ij} = -\alpha_{ij} n_i \partial T_i/\partial z$ are the thermal forces computed according to Ref. 20 for arbitrary concentrations of the charged particles, by assuming that the main ion mass m_i is much smaller than the impurity mass m: $\alpha_{ei} \approx n_i/(0.54 n_e + 0.87 n_i)$, $\alpha_{ej} \approx j^2 n_j/(0.54 n_e + 0.87 j^2 n_j)$, and $\alpha_{ij} \approx j^2 n_j/(0.38 n_i + 0.87 j^2 n_j)$.

Very often, impurity transport is considered in the so called trace limit presuming so low impurity concentrations that $n_{e,i}$ and $T_{e,i}$ are practically unperturbed. However, impurity neutrals usually enter into the plasma volume through small spots where their local density can be very high even for a relatively small absolute level of the impurity influx. Energy losses on excitation, ionization, and heating of produced ions in coulomb collisions can noticeably cool down the main plasma components near the impurity entrance position; their temperatures are governed by heat balance equations

$$\frac{3n_i}{2}\frac{\partial T_i}{\partial t} + T_i \frac{\partial \Gamma_i}{\partial z} - \frac{\partial}{\partial x}\left(\kappa_{ix}\frac{\partial T_i}{\partial x}\right) - \frac{\partial}{\partial y}\left(\kappa_{iy}\frac{\partial T_i}{\partial y}\right) - \frac{\partial}{\partial z}\left(\kappa_{iz}\frac{\partial T_i}{\partial z}\right) = 3n_i\left[k_{ei} n_e (T_e - T_i) + \sum_j k_{ij} n_j (T_j - T_i)\right], \tag{6}$$

$$\frac{3n_e}{2}\frac{\partial T_e}{\partial t} + T_e \frac{\partial \Gamma_e}{\partial z} - \frac{\partial}{\partial x}\left(\kappa_{ex}\frac{\partial T_e}{\partial x}\right) - \frac{\partial}{\partial y}\left(\kappa_{ey}\frac{\partial T_e}{\partial y}\right) - \frac{\partial}{\partial z}\left(\kappa_{ez}\frac{\partial T_e}{\partial z}\right) = n_e\left\{\sum_j n_j\left[3k_{ej}(T_j - T_e) - k_{ion}^j\left(I_j + \frac{3}{2}T_e\right) - L_j\right] + 3k_{ei}(T_i - T_e)n_i\right\}, \tag{7}$$

where Γ_e is the density of the electron particle flux along the magnetic field, $\kappa_{ix}, \kappa_{ex}, \kappa_{iy}, \kappa_{ey}, \kappa_{iz}$, and κ_{ez} are the components of heat conductions, I_j and L_j are the ionization energy and cooling rate of impurity ions, respectively. Temperature reduction near the impurity source leads to a parallel pressure gradient which drives a flow of the main ions along the magnetic field towards the source. The consequent change of the density n_i of the main ions is governed by the continuity equation

$$\frac{\partial n_i}{\partial t} - \frac{\partial}{\partial x}\left(D_x \frac{\partial n_i}{\partial x}\right) - \frac{\partial}{\partial y}\left(D_y \frac{\partial n_i}{\partial y}\right) + \frac{\partial \Gamma_i}{\partial z} = 0, \tag{8}$$

with the density of the ion parallel flux determined by the motion equation

$$m_i \frac{\partial \Gamma_i}{\partial t} - m_i \frac{\partial}{\partial x}\left(\frac{D_x}{n_i}\frac{\partial n_i}{\partial x}\Gamma_i\right) - m_i \frac{\partial}{\partial y}\left(\frac{D_y}{n_i}\frac{\partial n_i}{\partial y}\Gamma_i\right) + m_i \frac{\partial}{\partial z}\left(\frac{\Gamma_i^2}{n_i}\right) = -m_i \sum_j k_{ij}(n_j \Gamma_i - n_i \Gamma_j) - \frac{\partial (n_i T_i)}{\partial z} + e E_z n_i - F_{th}^{ei} + \sum_j F_{th}^{ij}. \tag{9}$$

In the initial state before impurity injection, the densities and temperatures of electrons and main ions are assumed identical and homogeneous, $n_{e,i}(t = 0, x, y, z) = n_*$ and $T_{e,i}(t = 0, x, y, z) = T_*$. At $t = 0$, the density of impurity neutrals is enhanced instantaneously in the source area, $x \le h_0$, $|y| \le \delta_0, |z| \le l_0$, to a level n_0 maintained constant later. The plasma parameters, being perturbed in the vicinity of the impurity source, approach to the values n_* and T_* far away from it. Equations (1)–(9) are strongly non-linearly coupled partial differential equations (PDEs). A straightforward integration of them is fraught with numerous sources for numerical instabilities, and as a first approximation, we apply henceforth an approach that allows to reduce the PDEs above to a set of ordinary differential equations (ODEs) for the time evolution of certain parameters characterizing the dependent variables of the problem in principal details.

III. "SHELL" APPROXIMATION

In the framework of the shell model, the whole space occupied by any particular charge state j of impurity is subdivided into the source, $x \le h_{s,j}, |y| \le \delta_{s,j}, |z| \le l_{s,j}$, where the j-ions are generated by the ionization of the $j-1$ ones and in the decay zone, $h_{s,j} < x, \delta_{s,j} < |y|, l_{s,j} < |z|$, where their density n_j drops due to the ionization into the $j+1$ state. For impurity ions in question of low charges, this behavior is formally reproduced with boundary conditions corresponding to zero y, z-derivatives of the densities at the

source center position, $y=z=0$, and $n_j \to 0$ far from the source, $x, |y|, |z| \to \infty$. The shape of the radial profiles is constructed by taking into account that outside the LCFS, charged particles escape to the wall and at $x=0$, a positive e-folding length for the density, $\lambda_j = dx/d\ln n_j$, is fixed. An approximate solution of Eq. (1) is presumed in the form $n_j(t,x,y,z) = n_j^0(t)\chi_j(t,x)\varphi_j(t,y)\psi_j(t,z)$ with

$$\chi_j(x \le h_{s,j}) = 1 - a_j(x - x_j)^2,$$
$$\chi_j(x > h_{s,j}) = [1 - a_j(h_{s,j} - x_j)^2]\exp\left(-\frac{x - h_{s,j}}{h_{d,j}}\right),$$

$$\varphi_j(|y| \le \delta_{s,j}) = 1 - \frac{\delta_{s,j}}{2\delta_{d,j} + \delta_{s,j}}\left(\frac{y}{\delta_{s,j}}\right)^2,$$
$$\varphi_j(\delta_{s,j} < |y|) = \frac{\delta_{d,j}}{\delta_{d,j} + \delta_{s,j}/2}\exp\left(-\frac{|y| - \delta_{s,j}}{\delta_{d,j}}\right),$$

$$\psi_j(|z| \le l_{s,j}) = 1 - \frac{l_{s,j}}{2l_{d,j} + l_{s,j}}\left(\frac{z}{l_{s,j}}\right)^2,$$
$$\psi_j(l_{s,j} < |z|) = \frac{l_{d,j}}{l_{d,j} + l_{s,j}/2}\exp\left(-\frac{|z| - l_{s,j}}{l_{d,j}}\right),$$

where $x_j = h_{s,j}(h_{s,j}/2 + h_{d,j})/(h_{s,j} + \lambda_j + h_{d,j})$ and $a_j = 1/(x_j^2 + 2\lambda_j x_j)$. Both the parameters x_j, a_j and the coefficients in functions φ_j and ψ_j have been found from the requirement that n_j and its first derivatives with respect to x, y, and z are continuous at the source boundary. In the of case Γ_j, one has to take into account that this reduces to zero at the axis $z=0$ and achieves its maximum at the source boundary, $z = l_{s,j}$. Therefore, $\Gamma_j(t,x,y,z) = \Gamma_j^0(t)\chi_j(t,x)\varphi_j(t,y)\chi_j(t,z)$ with $\chi_j(|z| \le l_{s,j}) = |z|/l_{s,j}$ and $\chi_j(l_{s,j} < |z|) = \exp[-(|z| - l_{s,j})/l_{d,j}]$. The functions $\chi_j, \varphi_j, \psi_j$, and χ_j are demonstrated in Fig. 2.

The impurity ion temperature is characterized by a single averaged value T_j in the whole shell occupied by j-ions that combines the source and decay regions

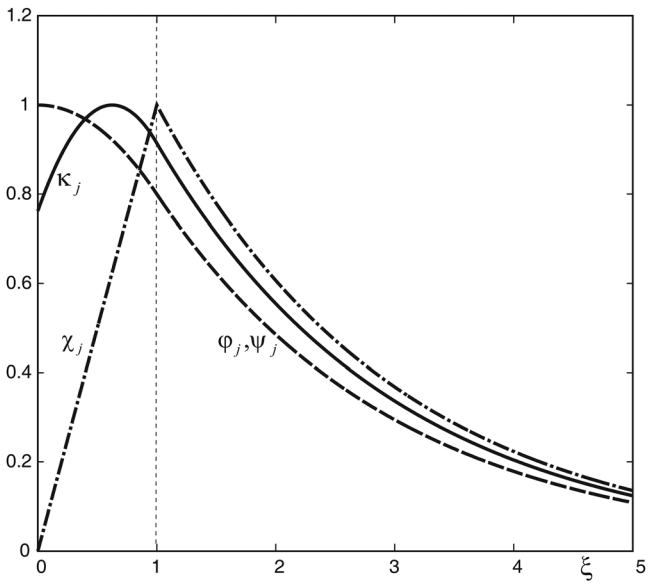

FIG. 2. The functions $\chi_j, \varphi_j, \psi_j$, and χ_j versus the dimensionless coordinate ξ equal to $x/h_{s,j}, y/\delta_{s,j}$, and $z/l_{s,j}$, correspondingly, for $h_{d,j}/h_{s,j} = \delta_{d,j}/\delta_{s,j} = l_{d,j}/l_{s,j} = 2$.

$$x \le h_j \equiv h_{s,j} + h_{d,j}, |y| \le \delta_j \equiv \delta_{s,j} + \delta_{d,j}, |z| \le l_j \equiv l_{s,j} + l_{d,j}.$$

Since the source region of the j-ions coincides with the total localization shell of the $j-1$ ones, the recurrent relations $h_{s,j} \approx h_{j-1}, \delta_{s,j} \approx \delta_{j-1}$, and $l_{s,j} \approx l_{j-1}$ are assumed. In the decay region of j-ions, $h_{s,j} < x < h_j$, $\delta_{s,j} < |y| < \delta_j$, and $l_{s,j} < |y| < l_j$, both the temperatures of electrons and main ions and the density of the latter are approximated by step functions with spatially homogeneous but time dependent values $T_{e,j}, T_{i,j}$, and $n_{i,j}$, respectively. In this region, the j-ions dominate the impurity contribution to the electron density, i.e.,

$$n_e \approx n_{i,j} + jn_j.$$

The determination of the time variation of the parameters $h_{d,j}, \delta_{d,j}, l_{d,j}, n_j^0, \Gamma_j^0, T_j, T_{e,j}, T_{i,j}$, and $n_{i,j}$ is the main purpose of the "shell" approximation. Let us start with $h_{d,j}, \delta_{d,j}, l_{d,j}$, and n_j^0. To find equations for these, the solution in the form assumed above is substituted into Eq. (1) and both sides of the latter are integrated over four regions in the (x, y, z)-space: the total shell, $0 \le x, |y|, |z| < \infty$; the x-region, $h_{s,j} \le x, 0 \le |y|, |z| < \infty$; the y-region, $0 \le x, \delta_{s,j} \le |y| < \infty, 0 \le |z| < \infty$; and the z-region, $0 \le x, |y| < \infty, l_{s,j} \le |z| < \infty$. The projections of these regions on the (y, z)-plane is shown in Fig. 2 of Ref. 10. The integration procedure provides the following ODEs:

$$dN_{w,j}/dt = N_{w,j-1}k_{ion}^{j-1}n_{ew,j-1} - N_{w,j}(k_{ion}^j n_{ew,j} + \nu_j), \quad (10)$$

$$dN_{x,j}/dt = (D_x/h_{d,j}^2 - k_{ion}^j n_{ex,j})N_{x,j}, \quad (11)$$

$$dN_{y,j}/dt = (D_x/\delta_{d,j}^2 - k_{ion}^j n_{ey,j} + \nu_j)N_{y,j}, \quad (12)$$

$$dN_{z,j}/dt = G_j/[ml_{s,j}(0.5 + I_{z11})] - (k_{ion}^j n_{ez,j} + \nu_j)N_{z,j}, \quad (13)$$

where $N_{w,j} = n_j^0 h_{s,j}\delta_{s,j}\ l_{s,j}I_{x1}I_{y1}I_{z1}, N_{x,j} = N_{w,j}I_{x11}/I_{x1}$, $N_{y,j} = N_{w,j}I_{y11}/I_{y1}$, and $N_{z,j} = N_{w,j}I_{z11}/I_{z1}$ are the whole numbers of j-ions in the regions in question with $I_{x1} = I_{x01} + I_{x11}$, $I_{x2} = I_{x02} + I_{x12}$, $I_{y1} = I_{y01} + I_{y11}$, $I_{y2} = I_{y02} + I_{y12}$, $I_{z1} = I_{z01} + I_{z11}$, $I_{z2} = I_{z02} + I_{z12}$, $I_{x01} = 1 - a_j\left[h_{s,j}^2/3 - x_j(h_{s,j} - x_j)\right]$, $I_{x11} = \xi_x[1 - a_j(h_{s,j} - x_j)^2]$, $I_{x02} = 2I_{x01} - 1 + a_j^2\left[(h_{s,j} - x_j)^5 - x_j^5\right]/(5h_{s,j})$, $I_{x12} = I_{x11}^2/(2\xi_x)$, $I_{y01} = 1 - \delta_{s,j}/(6\delta_j)$, $I_{y11} = 2\xi_y^2/(1 + 2\xi_y)$, $I_{y02} = 1 - 2/(3 + 6\xi_y) + 1/\left[5(1 + 2\xi_y)^2\right]$, $I_{y12} = I_{y11}^2/(2\xi_y)$, $I_{z01} = 1 - l_{s,j}/(6l_j)$, $I_{z11} = 2\xi_z^2/(1 + 2\xi_z)$, $I_{z02} = 1 - 2/(3 + 6\xi_z) + 1/\left[5(1 + 2\xi_z)^2\right]$, $I_{z12} = I_{z11}^2/(2\xi_z)$, $\xi_x = h_{d,j}/h_{s,j}, \xi_y = \delta_{d,j}/\delta_{s,j}, \xi_z = l_{d,j}/l_{s,j}, n_{ew,j} = n_{i,j} + n_j^0 I_{x2}I_{y2}I_{z2}/(I_{x1}I_{y1}I_{z1})$, $n_{ex,j} = n_{i,j} + n_j^0 I_{x12}I_{y2}I_{z2}/(I_{x11}I_{y1}I_{z1})$, $n_{ey,j} = n_{i,j} + n_j^0 I_{x2}I_{y12}I_{z2}/(I_{x1}I_{y11}I_{z1})$, $n_{ez,j} = n_{i,j} + n_j^0 I_{x2}I_{y2}I_{z12}/(I_{x1}I_{y1}I_{z11})$. The frequency $\nu_j = 2D_x a_j x_j/[h_{s,j}(I_{x01} + I_{x11})]$ characterizes the loss of the j-ions through the LCFS. The original dependent variables of the "shell" model, $h_{d,j}, \delta_{d,j}, l_{d,j}$, and n_j^0, can be explicitly expressed through $N_{w,j}, N_{x,j}, N_{y,j}$, and $N_{x,j}$. The following relationships have been obtained from the definitions above:

$$h_{d,j} = h_{s,j}\frac{h_{s,j}/3+\lambda_j+\sqrt{(h_{s,j}/3+\lambda_j)^2+(h_{s,j}+2\lambda_j)(h_{s,j}/6+\lambda_j)(N_{w,j}/N_{x,j}-1)}}{(h_{s,j}+2\lambda_j)(N_{w,j}/N_{x,j}-1)}, \tag{14}$$

$$\delta_{d,j} = \frac{\delta_{s,j}}{2}\frac{1+\sqrt{(4N_{w,j}/N_{y,j}-1)/3}}{N_{w,j}/N_{y,j}-1}, \qquad l_{d,j} = \frac{l_{s,j}}{2}\frac{1+\sqrt{(4N_{w,j}/N_{z,j}-1)/3}}{N_{w,j}/N_{z,j}-1}. \tag{15}$$

In Eq. (13), $G_j \equiv m\Gamma_j^0 h_{s,j}\delta_{s,j}l_{s,j}I_{x1}I_{y1}(1/2+I_{z11})$ is the total parallel momentum of impurity j-ions. The integral of Eq. (3) over the whole shell, with Eq. (5) taken into account, provides an equation for G_j

$$dG_j/dt = f_j N_{w,j} - \nu_G^j G_j, \tag{16}$$

where $f_j \approx \frac{T_j+jT_{e,j}\left[1-\frac{n_{i,j}}{jn_j^0}\ln\left(1+\frac{jn_j^0}{n_{i,j}}\right)\right]}{l_{s,j}(I_{z01}+I_{z11})} - k_{ij}\Gamma_{i,j}m + f_{th}^j$, with $\Gamma_{i,j}$ being the density of the main ion parallel flux in the j-shell, and $\nu_G^j = k_{ij}n_{i,j} + k_{ion}^j n_{e\Gamma} + D_x/(\lambda_j h_{s,j}I_{x1})$, with $n_{e\Gamma} = n_{i,j} + n_j^0 I_{x2}I_{y2}\left(1/2 + a_j h_{s,j}^2/3 + I_{z12}\right)/\left[I_{x1}I_{y1}(1/2+I_{z11})\right]$, characterizes the diminishing of momentum by friction and ionization. In the approximation of step functions for the temperature profiles, the contribution in f_j from the thermal force is estimated as $f_{th}^j = j[\beta_{ej}(T_{e,j}-T_{e,j-1}) + \beta_{ij}(T_{i,j}-T_{i,j-1})]/(I_{x1}I_{y1}I_{z1})$, with $\beta_{ej} \approx [0.54/j + (0.54+0.87j)n_j^0/n_{i,j}]^{-1} - (1.41+0.54jn_j^0/n_{i,j})^{-1}$ and $\beta_{ij} \approx (0.38/j + 0.87jn_j^0/n_{i,j})^{-1}$. One can see that this contribution approaches to zero in two important limit cases: (i) of small impurity content, $n_j^0/n_{i,j} \ll 1$, where temperature gradients along magnetic field vanishes and $T_{e,j} \approx T_{e,j-1}$, $T_{i,j} \approx T_{i,j-1}$; (ii) of large impurity concentration, $n_j^0/n_{i,j} \gg 1$, where $\beta_{ej}, \beta_{ij} \to 0$ and the thermal forces are inefficient. Therefore, we expect that the thermal force impact is in any case moderate and does affect the results noticeably, unlike the situation in the SOL of a tokamak with strong recycling in divertor where a significant temperature gradient is present even without impurity.[18] Unfortunately, this expectation cannot be validated by calculations in this paper since in the case of singly charged impurity ions, considered quantitatively below, $f_{th}^1 = 0$.

The integration of the heat balance equation (4) over the whole j-shell results in the following equation for the time evolution of the characteristic temperature of impurity ions:

$$dT_j/dt = (T_{j-1}-T_j)k_{ion}^{j-1}n_{ew,j-1}N_{w,j-1}/N_{w,j} + 2k_{ij}n_{i,j}(T_{i,j}-T_j) + 2k_{ej}n_{ew,j}(T_{e,j}-T_j). \tag{17}$$

Equations for the parameters $T_{e,j}, T_{i,j}$, and $n_{i,j}$ are formulated below for $j=1$ only. Although this limitation of the present model will be withdrawn in future, the present reduced description is of direct relevance for such important impurities as helium and lithium. Both species are used in fusion for diagnostic purposes. In addition, He is a product of thermonuclear reactions and Li is utilized as a plasma facing material. The $j=2$ ions of helium are completely stripped and spread out over the whole magnetic surfaces. The ionization energy of doubly charged lithium ions is of 122.5 eV and at the plasma edge with an electron temperature of several tens of eV, they disappear very slowly and also have enough time for spreading out over the magnetic surfaces. Moreover, our previous study[10] has demonstrated that even for argon impurity, whose charge states with $j \geq 2$ have much lower ionization energies, these do not contribute visibly to n_e up to extremely high injection rates being unrealistic for many applications. As one can presume from the results of stationary analysis for singly charged carbon ions[9] and estimates done for argon in Ref. 10, even higher impurity densities are necessary to change T_e, T_i, and n_i noticeably.

For the temperatures of the main plasma components in the shell of singly charged impurity ions, we have got the following equations:

$$1.5N_{i,1}dT_{i,1}/dt = 3n_{i,1}[k_{ei}(N_{i,1}+N_{w,1})(T_{e,1}-T_{i,1}) + k_{i1}N_{w,1}(T_1-T_{i,1})] + Q_{i,1}, \tag{18}$$

$$\begin{aligned}1.5(N_{i,1}+N_{w,1})dT_{e,1}/dt = {} & 3n_{i,1}k_{ei}(N_{i,1}+N_{w,1})(T_{i,1}-T_{e,1}) \\ & +3n_{ew,1}k_{e1}N_{w,1}(T_1-T_{e,1}) \\ & -n_{e,0}N_0[k_{ion}^0(I_0+1.5T_{e,1})+L_0] \\ & -n_{ew,1}N_{w,1}[k_{ion}^1(I_1+1.5T_{e,1})+L_1] \\ & +Q_{e,1},\end{aligned} \tag{19}$$

where $N_0 = n_0 h_0 \delta_0 l_0, N_{i,1} = n_{i,1}h_1\delta_1 l_1$, and $n_{e,0} = n_{i,1} + n_1^0 I_{x01}I_{y01}I_{z01}$; $Q_{i,1}$ and $Q_{e,1}$ are the total heat influxes into the shell of singly charged impurity ions transported from distant plasma regions by the heat conductions of the main ions and electrons, respectively. These are evaluated according to the approach developed in Ref. 9. The density of the main ions in the shell in question is governed by the equation

$$dN_{i,1}/dt = \nu_{i\perp}(n_* h_1\delta_1 l_1 - N_{i,1}) + h_1\delta_1\Gamma_{i,1}. \tag{20}$$

Here, the rhs gives the particle supply due to flows both perpendicular, the first term, and parallel, the second one, to the magnetic field from the distant plasma where the unperturbed density n_* and temperatures T_{e*} and T_{i*} are maintained. The frequency $\nu_{i\perp}$ characterizes the perpendicular transport induced by the deviation of n_i from n_* beyond the $j=1$ shell and is adopted as a free parameter. We have found that in a wide range of physically reasonable values of $\nu_{i\perp}$, up to $10^5\ s^{-1}$, the results of calculations are very insensitive to its absolute magnitude. The parallel flux density $\Gamma_{i,1}$ is assessed according to Ref. 21 and is governed by the following equation:

$$d\Gamma_{i,1}/dt = [n_*(T_{e*} + T_{i*}) - n_{i,1}(T_{e,1} + T_{i,1})]/(m_i L) - \Gamma_{i,1}^2/(n_{i,1}L) - \nu_{i\perp}\Gamma_{i,1}, \quad (21)$$

where L is the characteristic length of a field line, connecting the impurity cloud and distant plasma.

IV. RESULTS OF CALCULATIONS

"Shell" model equations above have been used to study the dynamics of spreading of singly charged lithium ions at the edge of a deuterium plasma in a tokamak device. In the initial state before impurity injection, the identical densities and temperatures of electrons and deuterons are $n_* = 10^{19}\,\mathrm{m}^{-3}$ and $T_* = 50$ eV, respectively. During injection, the parameters of the main plasma components far from the impurity source are assumed approaching to their unperturbed levels n_* and T_*. For the perpendicular diffusivity components, we adopted $D_{x,y} = 1\ \mathrm{m}^2\mathrm{s}^{-1}$. The temperature dependences of the ionization rate coefficients k_{ion}^j and cooling rates L_j for lithium atoms and ions have been taken from Refs. 22 and 23. Figures 1 and 2 show the time evolution of the parameters $\delta_1, l_1, n_1^0, n_i, T_1, T_e$, and T_i in the shell of singly charged lithium ions. Calculations have been done for two close magnitudes of the impurity atom density n_0 by assuming that *Li*-atoms are localized in the source region with the dimensions $h_0 = 0.01\,\mathrm{m}, \delta_0 = l_0 = 0.01\,\mathrm{m}$ and have a temperature T_0 of 0.03 eV.

For $n_0 = 0.75 \cdot 10^{19}\,\mathrm{m}^{-3}$, Fig. 3, the initial transient cooling of electrons is not supported by the main ions. Finally, owing to heating in collisions with the main ions, remaining hot, T_e relaxes to a level comparable with the initial one. Both excitation of impurity ions and coulomb collisions with them are not efficient to preserve electron cooling because n_1 is limited at a low enough level: in collisions with the main ions, the impurity ones are heated up and their pressure gradient and the electric field dissolve them on a distance l_1 of several meters along the magnetic field. In the case of a slightly higher $n_0 = 10^{19}\,\mathrm{m}^{-3}$, Fig. 4, a compact bubble of very dense and cold plasma, with a dimension l_1 of several centimeters along the magnetic field, develops. Impurity ions are confined in this structure by the friction with the main ones and their density n_1 and, thus, n_e exceed the initial plasma density n_* by two orders of magnitude. The

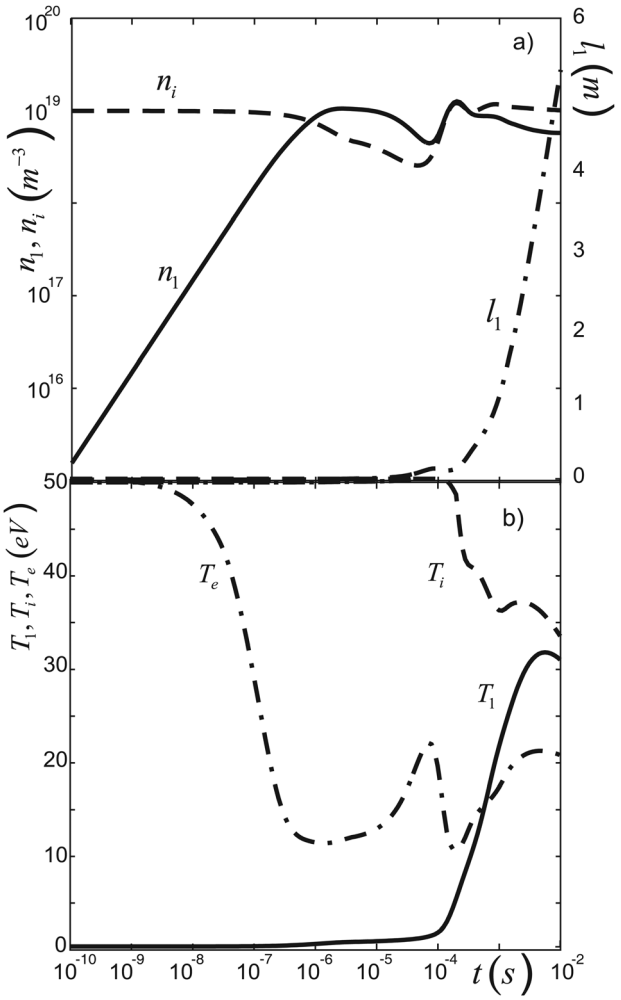

FIG. 3. Time evolution of the densities of singly charged lithium ions (solid curve) and main deuterons (dashed curve), the parallel extension of the Li^+-shell (dashed-dotted curve) (a) and of the temperatures of the Li^+-ions (solid curve), the main ions (dashed curve), and electrons (dashed-dotted curve) (b) computed for the density n_0 of lithium atoms of $0.75 \cdot 10^{19}\,\mathrm{m}^{-3}$.

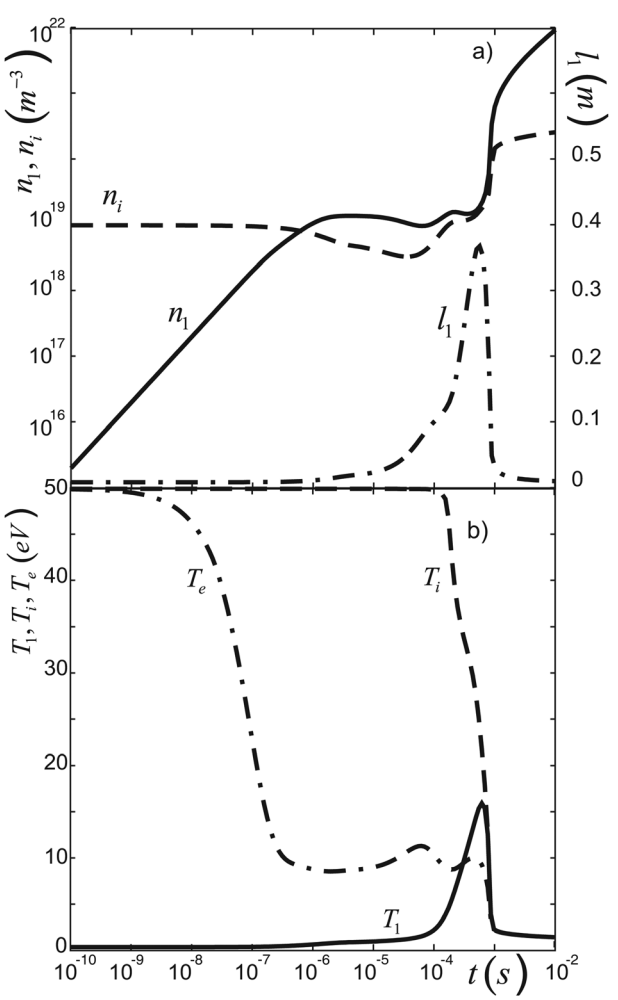

FIG. 4. Time evolution of the densities of singly charged lithium ions (solid curve) and main deuterons (dashed curve), the parallel extension of the Li^+-shell (dashed-dotted curve) (a) and of the temperatures of the Li^+-ions (solid curve), the main ions (dashed curve), and electrons (dashed-dotted curve) (b) computed for the density n_0 of lithium atoms of $10^{19}\,\mathrm{m}^{-3}$.

final state cannot be, however, consistently described in the framework of the present model because it does not account for recombination processes and radiation opacity being important under such conditions.

Normally condensation phenomena like that demonstrated in Fig. 4 are thought to be triggered by electron energy losses on excitation of impurity and radiated away. Our present model includes in addition to this loss channel also coulomb collisions between different plasma components. This allows to analyse which mechanisms are of the most importance for the condensation and structure development. Figure 5 displays the time evolution of parameters computed under different assumptions for $n_0 = 1.5 \cdot 10^{19}\,\mathrm{m}^{-3}$. One can see that in the case without radiation losses, the dashed-dotted curves, the cooling phase continues longer but finally after a time of $1\mu s$ condensation also develops. In this case, the background plasma is cooled down by heat transfer to cold impurity ions in coulomb collisions. For the case of a homogeneous plasma, the dominance of this energy loss channel over radiation has been already mentioned in Ref. 24. However, for the formation of compact structures with cold dense plasma not only heat transfer between charged components but also the friction force due to coulomb collisions between the main and impurity ions are of vital significance. This demonstrates the dashed-dotted curves in Fig. 5 computed with the friction between the ion components switched off: after a transient drop both T_i and T_e recover significantly and a compact cloud of cold dense plasma does not arise. These findings offer a new look on condensation instabilities and structure formation triggered in hot plasmas in the presence of impurities, differing principally from the standard explanation exploiting the effect of radiation losses.[25–29] Ion-ion coulomb collisions reduce the temperature of the main ions and the collision frequency rises as $T_i^{-1.5}$. Impurity ions are confined better near the entrance position since their friction with the main ones counteracts impurity dispersion by the pressure gradient and electric field. The impurity ion density and collision frequency grow up, and T_i drops further.

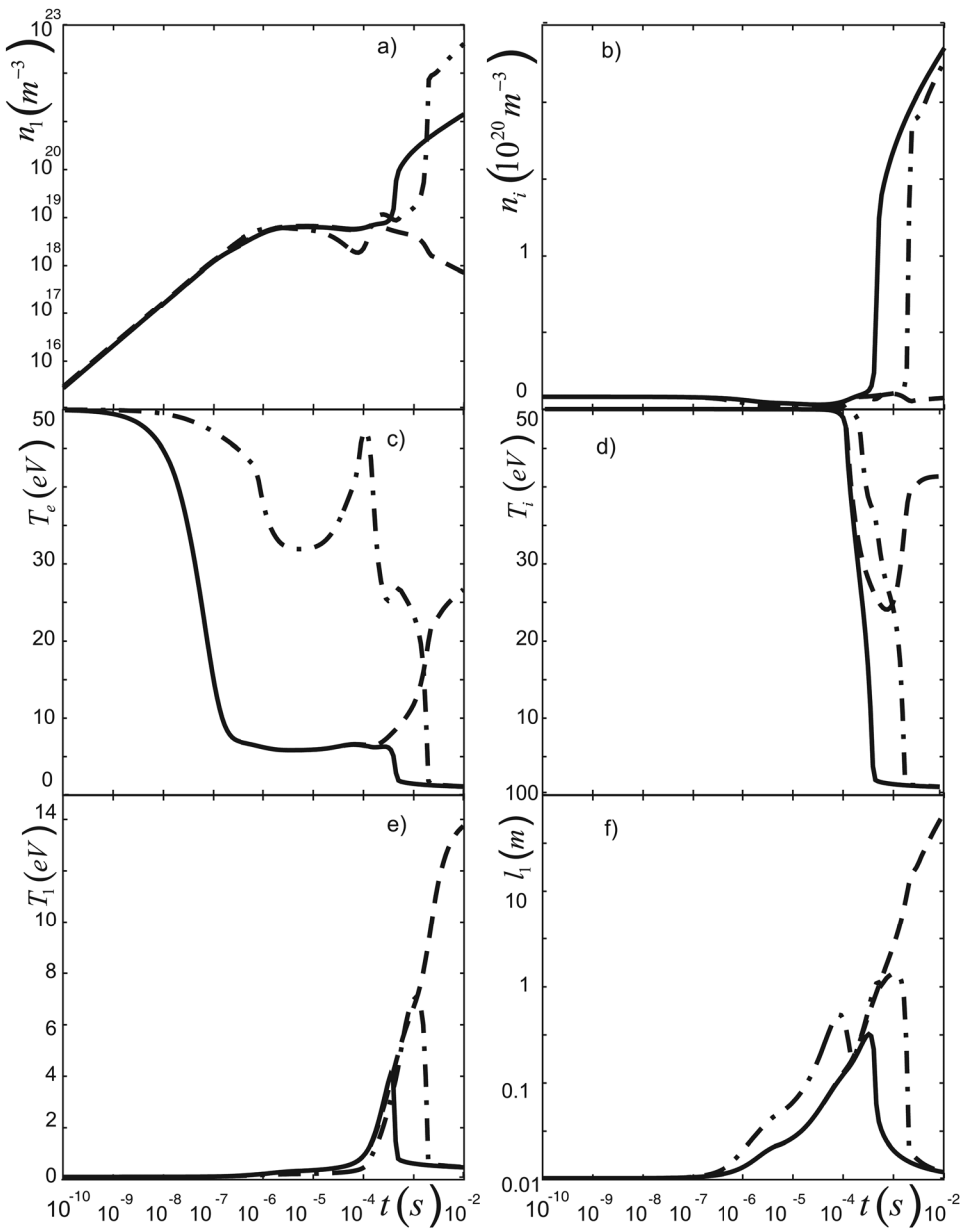

FIG. 5. Time evolution of the densities of singly charged Li impurity (a) and main (b) ions, the temperatures of electrons (c), deuterons (d), and Li^+ particles (e), and the extension of Li^+-shell along the magnetic field (f) computed for $n_0 = 1.5 \cdot 10^{19}\,\mathrm{m}^{-3}$, with all cooling mechanisms included (solid curves), without friction due to coulomb collisions between main and impurity ions (dashed curves) and without radiation energy losses (dashed-dotted curves).

This mechanism is enforced by the flow of the main ions towards the impurity source generated since the temperature reduction there results in dropping plasma pressure.

The transport of impurity ions perpendicular to the magnetic field both on the flux surfaces and across them is a topic in tokamak physics studied intensively during decades. In spite of enormous efforts, a sufficient understanding is got in special situations only, e.g., for the edge transport barrier in the H-mode with a low concentration of impurity treatable in a trace limit. In such a case, the surface averaged radial transport can be well interpreted in the framework of the so called neoclassical theory.[30] In plasmas dominated by turbulence, especially under conditions in question with impurity ion densities noticeably exceeding that of the main ions, the transport nature is still obscured. In the present paper, this transport channel is assumed to be purely diffusive and characterized by the same diffusivities in both perpendicular directions, $D_x = D_y = 1\,\mathrm{m}^2\,\mathrm{s}^{-1}$. To study how critical is this assumption for the results, these parameters have been varied by an order of magnitude, in the range $0.3 - 3\,\mathrm{m}^2\,\mathrm{s}^{-1}$. Fig. 6 demonstrates the time evolution of the characteristic density of singly charged impurity, n_1^0, and of the temperature of the main ions in the shell of Li^+ particles, computed with $n_0 = 1.5 \cdot 10^{19}\,\mathrm{m}^{-3}$ for three values of $D_x = D_y$. One can see that the results are only slightly different. This behavior is explained by the fact that the singly charged lithium ions have a relatively short life time and the motion along the magnetic field dominates the evolution of their density and, through coulomb collisions, of the main ion temperature. A higher level of impurity perpendicular transport is normally unrealistic in fusion devices.

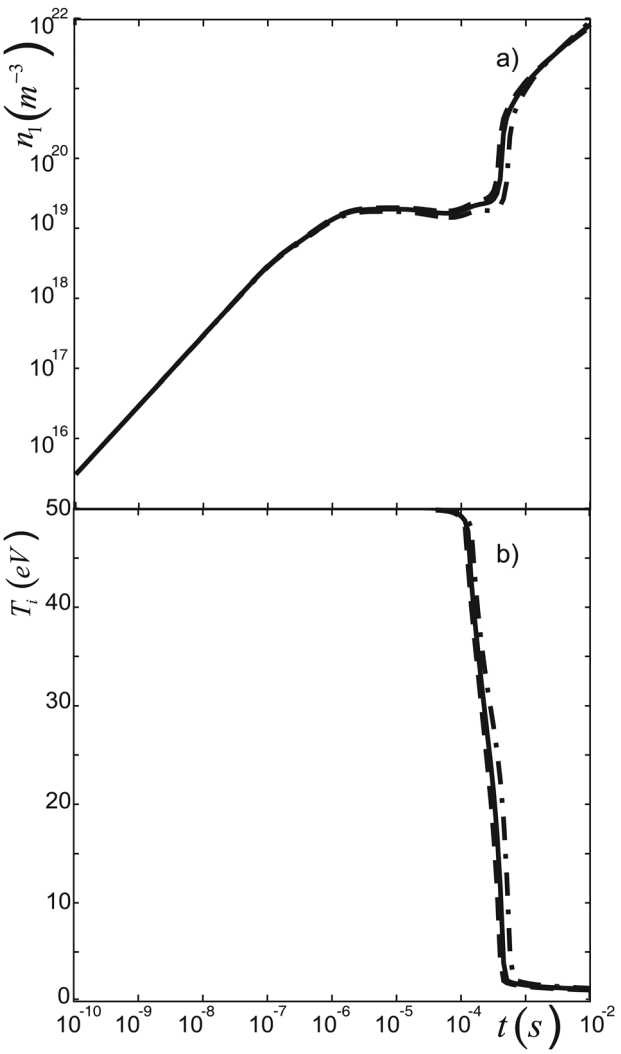

FIG. 6. Time evolution of the density of singly charged Li impurity (a) and the temperature of the main ions (b) computed for $n_0 = 1.5 \cdot 10^{19}\mathrm{m}^{-3}$, with different magnitudes of the perpendicular diffusivities $D_x = D_y$: 1 (solid curves), 0.3 (dashed curves), and $3\mathrm{m}^2\mathrm{s}^{-1}$ (dashed-dotted curves).

V. CONCLUSIONS

Diverse physical processes control the spreading of impurities from the injection position and the plasma response. These phenomena are interdependent and have to be described self-consistently. For this purpose, we elaborate a model where impurity ions of low charged states are considered as localized inside nested shells. These shells are subdivided into the source and decay regions, where the impurity ions of a particular charge are generated and disintegrated, respectively, in ionization processes. By integrating over such shells, three dimensional transport equations are reduced to a set of ordinary differential equations describing the time evolution of several characteristic parameters: the densities, temperatures of different impurity ion species, and dimensions of their shells along and across the magnetic field, and the densities and temperatures of the plasma main ions and electrons in these shells. As an example of applications, the spreading of lithium singly charged ions in deuterium plasma is numerically modelled. It is demonstrated that by exceeding a certain critical density of lithium neutrals, entering the plasma, a cooling condensation instability develops and a compact bubble structure with high densities and low temperatures of all plasma component arises and survives for a long time. It is shown that the cooling and friction of the main ions in coulomb collisions with impurity ones is the dominant mechanism among those responsible for the condensation phenomenon and structure formation. With decreasing temperature of the main ions, their friction with the impurity particles rises and counteracts the forces dispersing impurity ions from the injection position, namely, their own pressure gradient and the parallel electric field. The cooling of electrons through impurity radiation losses considered normally as the main instability cause cannot ensure a sustainable existence of structures. The proposed mechanism may be of relevance for the structure formation both in other laboratory plasmas and in interstellar medium.

ACKNOWLEDGMENTS

This work was partly supported by the German Research Foundation through the Research Training Group 1203.

[1]J. W. Coenen, V. Philipps, S. Brezinsek, B. Bazylev, A. Kreter, T. Hirai, M. Laengner, T. Tanabe, Y. Ueda, U. Samm, and the TEXTOR Team, Nucl. Fusion **51**, 083008 (2011).
[2]K. McCormick, S. Fiedler, G. Kocsis, J. Schweinzer, and S. Zoletnik, Fusion Eng. Des. **34–35**, 125 (1997).
[3]P. Wienhold, H. G. Esser, D. Hildebrandt, A. Kirschner, M. Mayer, V. Philipps, and M. Rubel, J. Nucl. Mater. **290–293**, 362 (2001).

[4]U. Samm, G. Bertschinger, P. Bogen, J. D. Hey, E. Hintz, L. Konen, Y. T. Lie, A. Pospieszczyk, D. Rusbuldt, R. P. Schorn, B. Schweer, M. Tokar, and B. Unterberg, Plasma Phys. Controlled Fusion **35**, B167 (1993).
[5]J. Ongena, A. M. Messiaen, M. Tokar, U. Samm, B. Unterberg, N. Schoon, P. Dumortier, H. G. Esser, F. Durodie, H. Euringer, G. Fuchs, E. Hintz, F. Hoenen, R. Koch, L. Könen, A. Krämer-Flecken, A. Pospieszczyk, B. Schweer, H. Soltwisch, G. Telesca, P. E. Vandenplas, R. van Nieuwenhove, G. van Oost, G. van Wassenhove, R. R. Weynants, G. Waidmann, J. Winter, and G. H. Wolf, Phys. Scr. **52**, 449 (1995).
[6]R. S. Granetz, E. M. Hollmann, D. G. Whyte, V. A. Izzo, G. Y. Antar, A. Bader, M. Bakhtiari, T. Biewer, J. A. Boedo, T. E. Evans, I. H. Hutchinson, T. C. Jernigan, D. S. Gray, M. Groth, D. A. Humphreys, C. J. Lasnier, R. A. Moyer, P. B. Parks, M. L. Reinke, D. L. Rudakov, E. J. Strait, J. L. Terry, J. Wesley, W. P. West, G. Wurden, and J. Yu, Nucl. Fusion **47**, 1086 (2007).
[7]D. Reiter, M. Baelmans, and P. Börner, Fusion Sci. Technol. **47**, 172 (2005).
[8]Y. Feng, F. Sardei, and J. Kisslinger, J. Nucl. Mater. **266–269**, 812 (1999).
[9]M. Koltunov and M. Z. Tokar, Plasma Phys. Controlled Fusion **53**, 065015 (2011).
[10]M. Koltunov and M. Z. Tokar, Plasma Phys. Controlled Fusion **54**, 025003 (2012).
[11]M. Z. Tokar and M. Koltunov, AIP Conf. Proc. **1389**, 1660 (2011).
[12]M. Z. Tokar, Nucl. Fusion **34**, 853 (1994).
[13]S. I. Krasheninnikov, Phys. Lett. A **283**, 368 (2001).
[14]B. LaBombard, J. W. Hughes, D. Mossessian, M. Greenwald, B. Lipschultz, J. L. Terry, and the Alcator C-Mod Team, Nucl. Fusion **45**, 1658 (2005).
[15]M. Z. Tokar, J. Comp. Phys. **230**, 2696 (2011).
[16]M. Z. Tokar, R. Ding, and M. Koltunov, Plasma Phys. Controlled Fusion **52**, 075003 (2010).
[17]G. M. McCracken *et al*., J. Nucl. Mater. **196–198**, 199–203 (1992).
[18]P. C. Stangeby, *The Plasma Boundary of Magnetic Fusion Devices* (Institute of Physics Publishing, Bristol, Philadelphia, 2000), pp. 277–357.
[19]S. I. Braginskii, "Transport Processes in a Plasma," in *Reviews of Plasma Physics*, edited by M. A. Leontovich (Consultants Bureau, New York, 1965), Vol. 1, pp. 205–311.
[20]S. Chapman, Proc. Phys. Soc., London, Sect. A **72**, 353 (1958).
[21]M. Z. Tokar, A. Gupta, D. Kalupin, and R. Singh, Plasma Phys. Controlled Fusion **49**, 395 (2007).
[22]K. L. Bell, H. B. Gilbody, J. G. Hughes, A. E. Kingston, and F. J. Smith, J. Phys. Chem. Ref. Data **12**, 891 (1983).
[23]J. Schweinzer, R. Brandenburg, I. Bray, R. Hoekstra, F. Aumayr, R. K. Janev, and H. P. Winter, At. Data Nucl. Data Tables **72**, 239–273 (1999).
[24]E. O. Baronova and V. V. Vikhrev, Contrib. Plasma Phys. **50**, 313 (2010).
[25]E. N. Parker, Astrophys. J. **117**, 431 (1953).
[26]G. B. Field, Astrophys. J. **142**, 531 (1965).
[27]B. Lipschultz, B. LaBombard, E. S. Marmar, M. M. Pickrell, J. L. Terry, R. Watterson, and S. M. Wolfe, Nucl. Fusion **24**, 977 (1984).
[28]J. F. Drake, Phys. Fluids **30**, 2429 (1987).
[29]W. M. Stacey, Plasma Phys. Controlled Fusion **39**, 1245 (1997).
[30]J. Wesson, *Tokamaks* (Oxford University Press, Inc., New York, 2004), p. 168.